

# Mesospheric temperature inversions observed in long-term lidar measurements at mid- and low-latitudes.

Thierry Leblanc, I. Stuart McDermid

Jet Propulsion Laboratory, California Institute of Technology, Table Mountain Facility, Wrightwood.

Philippe Keckhut, Alain Hauchecorne

Service d'Aéronomie du CNRS, Verrières-le-Buisson, France

**Abstract.** Results of an investigation of mesospheric temperature inversion layers using long-term lidar measurements at mid- and low-latitudes are reported. Observations of inversions above Table Mountain, California, (34.4°N) and Mauna Loa, Hawaii, (19.5°N) are in very good agreement with previous lidar and satellite observations. At least two distinct types of events have been observed. The winter inversions occur near 70 km altitude at midlatitudes in December-January and about 1-2 months later at subtropical latitudes. Also, some higher altitude inversions (80-85 km) have been observed at lower latitudes around the equinoxes and 1-2 months later at mid-latitudes. Several previously proposed mechanisms for the formation of these inversions are reviewed, including gravity wave breaking and tidal effects.

## 1. Introduction

Although not fully explained, mesospheric temperature inversion layers are frequently observed and identified. First reported by *Schmidlin* [1976], they are characterized by an inversion of the vertical temperature gradient in the mesosphere from negative to positive. The most striking events are usually observed at winter midlatitudes near 70 km with amplitudes (defined as the difference between the temperatures at the top and the bottom of the layer) reaching 40 K (e.g., [*Leblanc and Hauchecorne*, 1997]). Some inversion layers with weaker amplitudes were also observed at low- and midlatitudes near the equinoxes between 75 and 85 km by the Solar Mesospheric Explorer (SME) [*Clancy et al.*, 1994], the Improved Stratospheric And Mesospheric Sounder (ISAMS) and Halogen Occultation Experiment (HALOE) onboard UARS [*Leblanc and Hauchecorne*, 1997], and by lidar [*States and Gardner*, 1998]. At this time it is uncertain whether the higher altitude inversions and the lower altitude winter inversions have the same origin. *Leblanc and Hauchecorne* [1999] proposed a dynamical mechanism for the winter inversions at 70 km while chemical heating and tidal effects were proposed respectively by *Meriwether and Mlynczak* [1995] and by *States and Gardner* [1998] to explain their formation at 80-85 km.

In this paper, new results from different lidar observations of the inversion layers will be presented. Section 2 will briefly describe the lidar instruments and the database utilized. In sections 3 and 4, the observation of the inversions at mid- and lower latitudes will be reported and discussed.

## 2. Instruments and data sets

The results presented here have been obtained using temperature measurements from four ground-based Rayleigh lidars located at mid- and low-latitudes. The CNRS-Service d'Aéronomie lidar at the Observatoire de Haute-Provence, France (OHP,  $44^{\circ}\text{N}$ ,  $6.0^{\circ}\text{E}$ ) has operated since 1978 and a second lidar at the Centre d'Essais des Landes (CEL,  $44^{\circ}\text{N}$ ,  $1.0^{\circ}\text{W}$ ) was operated between 1986 and 1994. These lidars typically made measurements all night long (approximately 6 to 12 hours a night) on 4-5 nights a week depending on the season and weather permitting. The Jet Propulsion Laboratory (JPL) has operated lidars at the Table Mountain Facility, California (TMF,  $34.4^{\circ}\text{N}$ ,  $117.7^{\circ}\text{W}$ ) since 1988 and at Mauna Loa, Hawaii (MLO,  $19.5^{\circ}\text{N}$ ,  $155.6^{\circ}\text{W}$ ) since 1993. Both JPL lidars routinely make a 2 hour measurement early in the night, 4 nights a week, with some additional full night campaigns in 1996, 1997, and 1998.

These lidars transmit a laser into the atmosphere where it is Rayleigh backscattered by the air molecules. The intensity of the backscattered radiation received by a telescope on the ground is proportional to the number of molecules, i.e. the air density. The temperature is then deduced from the density using the classic hydrostatic equilibrium and ideal gas law assumptions. The potential 20 K total error at the top of the profiles (principally due to the use of a priori information and to the low signal at the top) decreases rapidly to a few Kelvins 10 km below, and to a few tenths of Kelvins 20 km below. The instrument specifications and principle have already been extensively documented (see for example, [Elterman, 1951; Hauchecorne and Chanin, 1980; McDermid *et al.*, 1995; and Leblanc *et al.*, 1998a]). Measurements from 1244 nights at OHP, 670 nights at CEL, 686 nights at TMF, and 411 nights at MLO were used to obtain the results presented below.

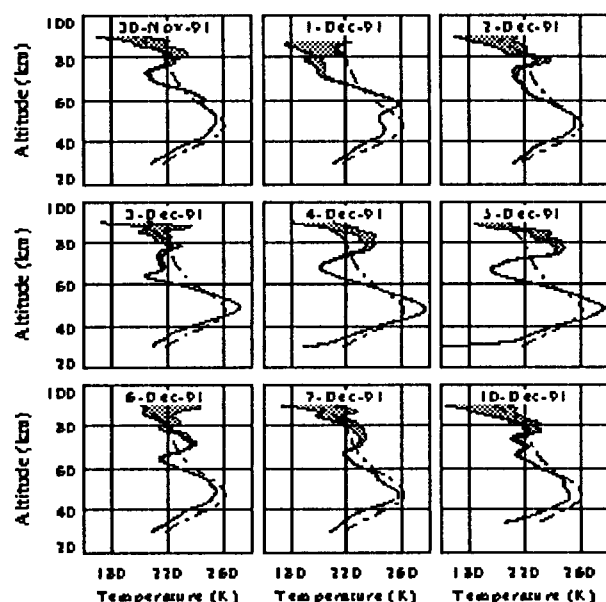


**Figure 1.** Nightly mean lidar temperature profiles between November 30 and December 10, 1991 at OHP ( $44.0^{\circ}\text{N}$ ).

Integration times run from 6 h 45 min to 12 h depending on weather conditions. The dashed line is the CIRA-86 profile.

### 3. Data analysis and results

**Figure 1** shows 9 nightly mean temperature profiles taken between December 1 and 10, 1991, at OHP (44°N). The shaded area represents the temperature plus and minus its calculated total error. The dashed lines indicate the monthly temperature climatology for December taken from CIRA-86 [Fleming *et al.*, 1990]. A strong temperature inversion can be seen to develop near 70 km starting on December 2, reaching an very large 55 K amplitude on December 5, then weakening and almost disappearing on December 10. This illustrates the magnitude and variability of such winter inversions. Lifetimes of a few hours to a few days have been reported [Leblanc and Hauchecorne, 1997].

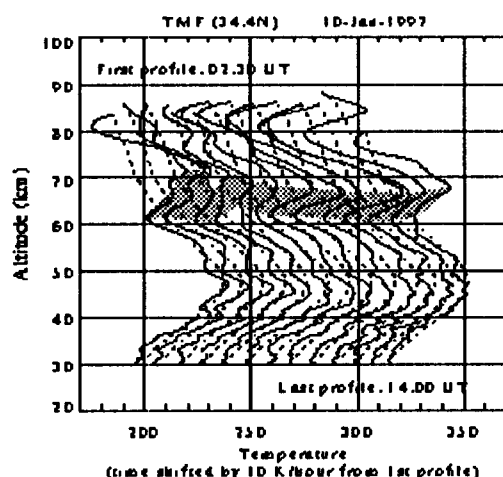


**Figure 2.** Hourly mean temperature profiles over TMF (34.4°N, 117°W) for January 10, 1997. Each profile is right-shifted by 10 K/hour, starting at 2:30 UT, ending at 14:00 UT. The dotted lines are the CIRA-86 climatology for January.

The nighttime evolution of a winter inversion at TMF (34.4°N) is illustrated in **Figure 2**. The temperature profiles are plotted every 1 hour and shifted by 10 K/hour to illustrate the time evolution. The first profile was taken at the very beginning of the night and the last profile at the very end. The total time separating the first and last profiles is approximately 12 hours. An important modulation of the amplitude (minimum of 10 K, maximum of 27 K) and an apparent downward propagation throughout the night are evident. These two characteristics are found almost every time. Occasionally (not shown here) the top of the inversion has been observed to propagate upward during short periods. The approximate downward phase speed of the inversion is 0.3 to 0.5 km/hour (8 to 14 cm.s<sup>-1</sup>). **Figure 3** shows the nighttime evolution of a temperature inversion observed at MLO (19.5°N) on October 10, 1996. In contrast to the winter inversions observed near 65-70 km at OHP and TMF, this inversion takes place near 80 km. The 40 K amplitude observed here is larger than the typical 10-20 K more

frequently observed at this altitude. However, a similar downward propagation throughout the night is clearly observed.

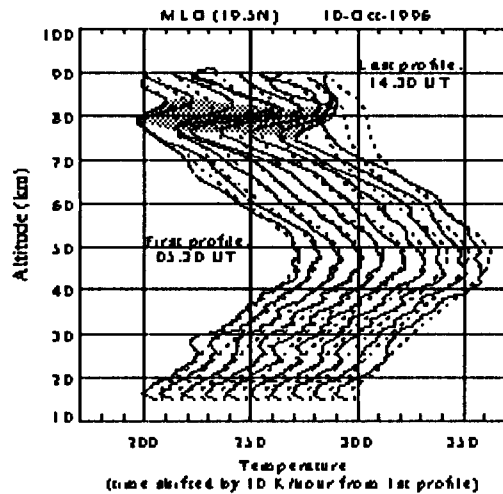


**Figure 3.** Same as figure 2, but at MLO (19.5°N, 155°W) for October 10, 1996. Starting and ending times are 5:30 UT and 14:30 UT

Plates 1a to 1d show the climatological average of the amplitude of the inversions as a function of altitude and season, observed at OHP (a) between 1984 and 1995, at CEL (b) between 1986 and 1994, at TMF (c) between 1990 and mid-1997, and at MLO (d) between mid-1993 and mid-1997. The altitude of the inversions is defined here as the center of the inversion layer. In order not to introduce errors due to the a priori initialization, the search for inversion layers was performed only up to about 10 km below the actual top of the profiles. This leads to top altitudes around 82 km for OHP, CEL, and MLO, and 78 km for TMF. At mid- and subtropical latitudes (i.e. OHP, CEL and TMF), the amplitude of the inversions at 70 km follows a well defined annual cycle with a maximum in winter. The winter maximum at TMF occurs 1 month later than at OHP and CEL (in January-February instead of December-January). This was already observed in the temperature climatology presented in [Leblanc *et al.*, 1998b] (see for example their plates 7a and 7b). At 80 km a larger but narrower maximum is observed in October-November that is well separated from the winter inversions, especially at OHP. Although also seen in the TMF results, this maximum is too high to be observable here. At MLO, the winter inversions are almost absent. Instead, a well defined semiannual cycle is observed at 80 km with maxima around the equinoxes. These results are in very good agreement with the satellite observations from SME [Clancy *et al.*, 1994], and ISAMS and HALOE [Leblanc and Hauchecorne, 1997].

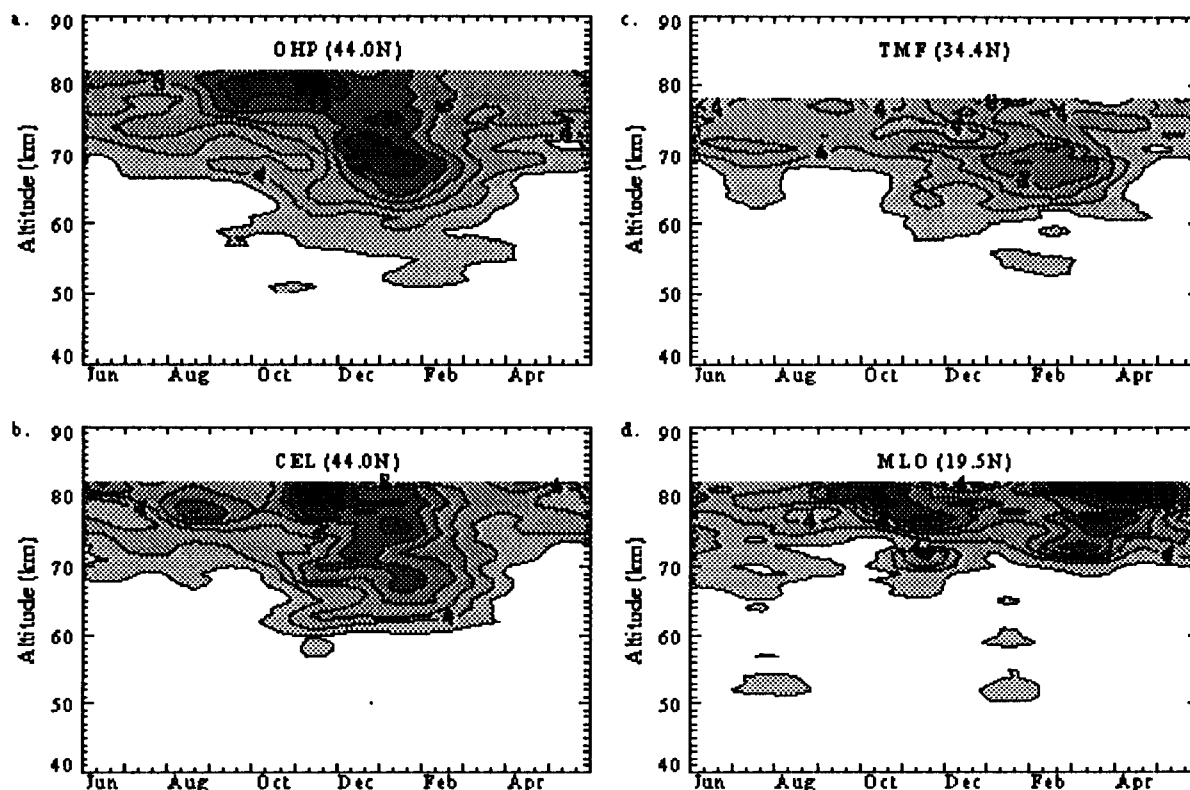


**Plate 1.** Monthly mean amplitude (K) of the mesospheric inversion layers as a function of season and altitude for a) OHP, b) CEL, c) TMF and d) MLO.

#### 4. Discussion and conclusion.

Figures 1 to 3 and plate 1 in this paper reveal two principal results:

1) The observations of the inversion layers above TMF (34.4°N) and MLO (19.5°N) are in very good agreement with the previous observations and climatologies obtained by lidar, SME and ISAMS and HALOE at similar latitudes.

2) There appear to be at least two distinct types of inversions:

- The first are the winter mid-latitude inversions occurring near 70 km altitude in December-January above OHP and CEL (44°N) and 1- to 2-months later above TMF (34.4°N). The winter inversions have previously been observed many times in both Northern and Southern hemispheres by SME, ISAMS and HALOE.

- The second type of inversions occurs at higher altitudes (80-85 km) at the equinoxes above MLO (19.5°N). Many inversion layers have also been observed at these altitudes and at the equinoxes by SME, ISAMS and HALOE at low latitudes, with a maximum amplitude at the equator.

- A possible third kind of inversion has been observed in October-November near 80 km above OHP, CEL, and TMF. These inversions appear to be well separated from those occurring at 70 km in winter and it is not clear whether they belong to the first type (winter midlatitude inversions) or to the second (equinox inversions), or even to a third type.

With regard to their vertical extent and amplitudes it would be tempting to interpret the mesospheric temperature

inversion layers as gravity wave disturbances. Their frequently observed downward phase speed would support this hypothesis. However, their lifetime of a few days is much longer than that of most of the gravity wave disturbances. Their short vertical scale makes them unlikely to be directly planetary wave related, including tides. Therefore, their origin is still a topic of debate. Basically, three different mechanisms have been suggested. Adiabatic heating and cooling due to gravity wave breaking was proposed by *Hauchecorne et al* [1987], and later by *Leblanc and Hauchecorne* [1999], to explain the formation of the winter midlatitude inversions. Following the calculations of *Mlynczak and Solomon* [1993], a chemical origin (exothermic reactions involving ozone and odd hydrogen) was suggested by *Meriwether and Mlynczak* [1995]. More recently *States and Gardner* [1998] proposed the tidal effect of two interacting out of phase diurnal modes to explain the so-called double-mesopause observed in several nighttime temperature climatologies of the mesopause region [*Yu and She*, 1995], and also to explain the presence of a downward propagating inversion layer around 85 km.

According to **figures 1 and 2**, pure gravity wave disturbances (of few hours period) are unlikely to be responsible for the winter inversion layers. Also, amplitudes of 40 K at 70 km and lifetimes of a few days do not seem to be compatible with the amplitudes and periods of mesospheric tides. In contrast, the role of gravity wave breaking and/or interaction between gravity waves and tides is consistent with all the observations (**figures 1 and 2** and **plates 1**), as well as with the previous observations by SME, ISAMS and HALOE, and with the temperature climatology by [*Leblanc et al.*, 1998b].

**Figure 3** and **plate 1** illustrate the presence of inversions at low-latitudes at the equinoxes in the region 80-85 km. Considering the altitudes at which they occur, their amplitudes, and due to the weak local Coriolis torque at these latitudes, it is more likely that they are caused by tidal and/or chemical effects rather than gravity wave breaking. Moreover, tidal models such as GSWM [*Hagan et al.*, 1995] predict a maximum in the diurnal amplitude near the equinoxes at lower latitudes. However, the downward propagation that would infer a tide related cause is not always observed as it appears in **Figure 3**.

Finally, **Plate 1** reveals the presence of inversions near 80 km at midlatitudes in October-November. Even though no inversions can be observed in our lidar profiles at altitudes higher than 82 km it is probable that they are closely related to those observed near 85 km in fall above Urbana (40°N) by *States and Gardner* [1998] who explained the formation of these inversions by the presence of two interacting diurnal modes. Although the propagating mode from the lower atmosphere has been successfully predicted by GSWM, an additional in-situ mode, out of phase with the upward propagating mode at 95 km, was not taken into account in the model. Only these new 24-hour Na-lidar measurements have revealed the behavior of the inversions at 85 km.

Although the mesospheric temperature inversion layers are still not fully explained, the recent and numerous observations have started to give some elements of an answer. Neither tidal

nor chemical origin is a satisfying explanation for the winter inversions because of their large amplitude for these low altitudes. Gravity wave breaking and/or interaction between gravity wave and tides may more likely be responsible. In contrast, the higher altitude inversions (85-90 km) occurring at lower latitudes during the equinoxes and at mid-latitudes 1-2 months later may be tidal related. Their observed seasonal variations and amplitudes are more consistent with the tidal theory. For both winter inversions and high altitude inversions it is probable that several mechanisms interact with each other. More temperature measurements in the mesosphere, in particular over full 24-hour cycles, are necessary to have a better understanding. The development of daytime lidar measurement techniques and long-term satellite measurements may bring new answers in the future.

**Acknowledgements.** The work described in this paper was carried out, in part, at the Jet Propulsion Laboratory, California Institute of Technology, under an agreement with the National Aeronautics and Space Administration. TL thanks the National Research Council for the award of an associateship. The long term measurements at OHP and CEL have been supported by DRET, CNES and INSU for CNRS.

## References

- Clancy, R. T., D. W. Rush, and M. T. Callan, Temperature minima in the average thermal structure of the middle atmosphere (70-80 km) from analysis of 40- to 92-km SME global temperature profiles, *J. Geophys. Res.*, **99**, 19,001-19,020, 1994.
- Elterman, L. B., The measurement of stratospheric density distribution with the searchlight technique, *J. Geophys. Res.*, **56**, 509-520, 1951.
- Fleming, E. L., S. Chandra, J. J. Barnett and M. Corney, COSPAR International Reference Atmosphere, Chapter 2: Zonal mean temperature, pressure, zonal wind and geopotential height as functions of latitude, *Adv. Space Res.*, **10** (12), 11-59, 1990.
- Hagan, M. E., J. M. Forbes and F. Vial, On modeling migrating solar tides, *Geophys. Res. Lett.*, **22**, 893-896, 1995.
- Hauchecorne, A., and M. L. Chanin, Density and Temperature Profiles obtained by lidar between 35 and 70 km, *Geophys. Res. Lett.*, **7**, 565-568, 1980.
- Hauchecorne, A., M. L. Chanin, and R. Wilson, Mesospheric temperature inversion and gravity wave breaking, *Geophys. Res. Lett.*, **14**, 933-936, 1987.
- Leblanc, T., and A. Hauchecorne, Recent observations of the mesospheric temperature inversions, *J. Geophys. Res.*, **102**, 19,471-19,482, 1997.
- Leblanc, T., I. S. McDermid, A. Hauchecorne, and P. Keckhut, Evaluation and optimization of lidar temperature analysis algorithms using simulated data, *in press J. Geophys. Res.*, 1998a.
- Leblanc, T., I. S. McDermid, C. Y. She, D. A. Krueger, A. Hauchecorne, and P. Keckhut, temperature climatology of the middle atmosphere from long-term lidar measurements at mid- and low-latitudes, *submitted J. Geophys. Res.*, 1998b.
- Leblanc, T., and A. Hauchecorne, 2-D numerical modeling of the mesospheric temperature inversions, *submitted, J. Atmos. Solar-Terr. Phys.*, 1999.
- McDermid, I. S., T. D. Walsh, A. Deslis and M. L. White, Optical systems design for a stratospheric lidar system, *Appl. Opt.*, **34**, 6201-6210, 1995.
- Meriwether, J. W., and M. G. Mlynczak, Is chemical heating a major cause of the mesosphere inversion layer ?, *J. Geophys. Res.*, **100**, 1379-1387, 1995.
- Mlynczak, M. G., and S. Solomon, A detailed evaluation of the heating efficiency in the middle atmosphere, *J. Geophys. Res.*, **98**, 10,517-10,541, 1993.

Schmidlin, F. J., Temperature inversions near 75 km, *Geophys. Res. Lett.*, **3**, 173-176, 1976.

States, R. J., and C. S. Gardner, Influence of the diurnal tide and thermospheric heat sources on the formation of mesospheric temperature inversion layers, *submitted*, *Geophys. Res. Lett.*, 1998.

Yu, J. R., and C. Y. She, Climatology of a midlatitude mesopause region observed by a lidar at Fort Collins, Colorado (40.6°N, 105°W), *J. Geophys. Res.*, **100**, 7441-7452, 1995.

---

T. Leblanc, I. S. McDermid, JPL-Table Mountain Observatory, P.O. Box 367, Wrightwood, CA, 92397. (e-mail: leblanc@tmf.jpl.nasa.gov)

A. Hauchecorne, P. Keckhut, Service d'Aéronomie du CNRS, BP 3, 91371 Verrières-le-Buisson, France.

Manuscript dates- Manuscript dates- Manuscript dates- Manuscript dates- Manuscript dates- Manuscript dates.

**Figure 1.** Nightly mean lidar temperature profiles between November 30 and December 10, 1991 over OHP (44.0°N). Integration times run from 6 h 45 min to 12 h depending on weather conditions. The dashed line is the CIRA-86 profile.

**Figure 2.** Hourly mean temperature profiles over TMF (34.4°N, 117°W) for January 10, 1997. Each profile is right-shifted by 10 K/hour, starting at 2:30 UT, ending at 14:00 UT. The dotted lines are the CIRA-86 climatology for January.

**Figure 3.** Same as figure 2, but over MLO (19.5°N, 155°W) for October 10, 1996. Starting and ending times are 5:30 UT and 14:30 UT

**Plate 1.** Monthly mean amplitude (K) of the mesospheric inversion layers as a function of season and altitude for a) OHP, b) CEL, c) TMF and d) MLO.